

# NASA Technical Memorandum 78709

(NASA-TM-78709) NASA LOW-AND MEDIUM-SPEED  
AIRFOIL DEVELOPMENT (NASA) 19 P  
HC A02/MF A01 CSCL 01C

N80-21294

Unclas  
G3/03 33612

## NASA Low- and Medium-Speed Airfoil Development

Robert J. McGhee, William D. Beasley,  
and Richard T. Whitcomb  
*Langley Research Center  
Hampton, Virginia*

**NASA**

National Aeronautics  
and Space Administration

**Scientific and Technical  
Information Office**

1979

REPRODUCED BY  
U.S. DEPARTMENT OF COMMERCE  
NATIONAL TECHNICAL  
INFORMATION SERVICE  
SPRINGFIELD, VA 22161



**U.S. DEPARTMENT OF COMMERCE**  
**National Technical Information Service**

N80-21294

NASA LOW- AND MEDIUM-SPEED AIRFOIL DEVELOPMENT

LANGLEY RESEARCH CENTER  
HAMPTON, VA

1979



1. Report No. NASA TM-78709	2. Government Accession No.	3. Recipient's Catalog No.	
4. Title and Subtitle NASA LOW- AND MEDIUM-SPEED AIRFOIL DEVELOPMENT		5. Report Date March 1979	
		6. Performing Organization Code	
7. Author(s) Robert J. McGhee, William D. Beasley, and Richard T. Whitcomb		8. Performing Organization Report No. L-12264	
		10. Work Unit No. 505-06-33-10	
9. Performing Organization Name and Address NASA Langley Research Center Hampton, VA 23665		11. Contract or Grant No.	
		13. Type of Report and Period Covered Technical Memorandum	
12. Sponsoring Agency Name and Address National Aeronautics and Space Administration Washington, DC 20546		14. Sponsoring Agency Code	
		15. Supplementary Notes This paper was presented at the NASA Conference on Advanced Technology Airfoil Research held at Langley Research Center on March 7-9, 1978, and is published in NASA CP-2046.	
16. Abstract  The status of NASA low- and medium-speed airfoil research, which was initiated in 1972 with the development of the GA(W)-1 airfoil and which has now emerged as a family of airfoils, is discussed. Effects of airfoil thickness-chord ratios varying from 9 percent to 21 percent on the section characteristics for a design lift coefficient of 0.40 are presented for the initial low-speed family of airfoils. Also, modifications to the 17-percent low-speed airfoil to reduce the pitching-moment coefficient and to the 21-percent low-speed airfoil to increase the lift-drag ratio are discussed. Representative wind-tunnel results are shown for two new medium-speed airfoils with thickness ratios of 13 percent and 17 percent and design-lift coefficients of 0.30. These new airfoils were developed to increase the cruise Mach number of the low-speed airfoils while retaining good high-lift, low-speed characteristics. Applications of NASA-developed airfoils to general aviation aircraft are summarized.			
17. Key Words (Suggested by Author(s)) Low-speed airfoils Medium-speed airfoils Thickness effects Reynolds number effects Mach number effects			
19. Security Classif. (of this report) Unclassified	20. Security Classif. (of this page) Unclassified	21. No. of Pages 16	22. Price

~~Available from NASA's Industrial Application Centers~~

NASA-Langley, 1979

111

ORIGINAL PAGE IS  
OF POOR QUALITY



## SUMMARY

The status of NASA low- and medium-speed airfoil research, which was initiated in 1972 with the development of the GA(W)-1 airfoil and which has now emerged as a family of airfoils, is discussed. Effects of airfoil thickness-chord ratios varying from 9 percent to 21 percent on the section characteristics for a design lift coefficient of 0.40 are presented for the initial low-speed family of airfoils. Also, modifications to the 17-percent low-speed airfoil to reduce the pitching-moment coefficient and to the 21-percent low-speed airfoil to increase the lift-drag ratio are discussed. Representative wind-tunnel results are shown for two new medium-speed airfoils with thickness ratios of 13 percent and 17 percent and design lift coefficients of 0.30. These new airfoils were developed to increase the cruise Mach number of the low-speed airfoils while retaining good high-lift, low-speed characteristics. Applications of NASA-developed airfoils to general aviation aircraft are summarized.

## INTRODUCTION

Research on advanced technology airfoils for low-speed general aviation applications has received considerable attention at Langley since the development of the GA(W)-1 airfoil in 1972. This airfoil was analytically developed using the subsonic viscous computer code of reference 1 which provided a low-cost analysis of the airfoil performance. References 2 and 3 report the experimental results for this airfoil and others derived from it, and references 4 to 6 report flap and control-surface results for several of these airfoils. Flight test results for the GA(W)-2 airfoil are reported in reference 7.

This research effort was initially generated to develop advanced airfoils for low-speed applications. Emphasis was placed on designing airfoils with largely turbulent boundary layers which had the following performance requirements: low cruise drag, high climb lift-drag ratios, high maximum lift, and predictable, docile stall behavior. However, in 1976 the need developed for airfoils with higher cruise Mach numbers than the low-speed airfoils provided, while retaining good high-lift, low-speed characteristics. Thus, two medium-speed airfoils were developed. These medium-speed airfoils are intended to fill the gap between the low-speed airfoils and the supercritical airfoils for application on light executive-type aircraft. In this paper the status of low- and medium-speed airfoil research is discussed and the applications of NASA-developed airfoils to general aviation aircraft are summarized.

## SYMBOLS

$C_p$	pressure coefficient
$c$	airfoil chord
$c_d$	section drag coefficient
$c_l$	section lift coefficient
$c_m$	section quarter-chord pitching-moment coefficient
$l/d$	section lift-drag ratio
$M$	Mach number
$R$	Reynolds number
$t$	airfoil thickness
$x$	airfoil abscissa
$\alpha$	angle of attack

### Subscripts:

$d$	design
$max$	maximum
$SEP$	separation
$T$	transition

## AIRFOIL DESIGNATION

Sketches of the section shapes and airfoil designations for the low- and medium-speed airfoils are shown in figure 1. The airfoils are designated in the form LS(1)- or MS(1)-xxxx. LS(1) indicates low speed (first series) and MS(1) indicates medium speed (first series); the next two digits designate the airfoil design lift coefficient in tenths, and the last two digits are the airfoil thickness in percent chord. Thus, the GA(W)-1 airfoil becomes LS(1)-0417 and the GA(W)-2 airfoil becomes LS(1)-0413.

## LOW-SPEED AIRFOILS

### Initial Family

This initial family of low-speed airfoils was obtained by linearly scaling the mean thickness distribution of the 17-percent airfoil (LS(1)-0417).



Thus, all four airfoils have the same camber distribution and the design lift coefficient is 0.40. The effects of varying thickness-chord ratio from 9 to 21 percent on maximum lift coefficient and lift-drag ratio are shown in figure 2 for a Reynolds number of  $4 \times 10^6$  with transition fixed near the leading edge of the airfoils. The maximum lift coefficient increases with thickness ratio up to a thickness ratio of about 13 percent; further increase in thickness ratio results in a decrease in maximum lift coefficient. For the 13-percent airfoil a value of maximum lift coefficient of about 1.9 is indicated. The lift-drag ratio decreases almost linearly with increasing thickness ratio over the entire thickness-ratio range at the design lift coefficient of 0.40. This decrease in lift-drag ratio is essentially a result of increased skin-friction drag because of the higher induced velocities for the thicker airfoils. However, at a typical climb lift coefficient of 1.0, this linear variation is indicated only up to a thickness ratio of about 17 percent. The large decrease in lift-drag ratio for the 21-percent airfoil is indicative of excessive turbulent boundary-layer separation. This effect has been reduced by redesign of the airfoil and is discussed later.

The scale effects on maximum lift coefficient for the low-speed airfoils for Reynolds numbers from about  $2 \times 10^6$  to  $9 \times 10^6$  are shown in figure 3. Increases in Reynolds number have a favorable effect on maximum lift coefficient for all thickness ratios shown. The increment in maximum lift coefficient with Reynolds number generally increases with increasing thickness ratio; however, note the differences in variation with Reynolds number. Application of a roughness strip just sufficient to trip the boundary layer resulted in only small effects on maximum lift coefficient for the 9- and 13-percent airfoils; however, large decreases occurred for the thicker airfoils.

Comparison of the maximum lift coefficients for this low-speed family with the older NACA airfoils is shown in figure 4 at a Reynolds number of  $6 \times 10^6$  for the airfoils smooth. The comparison is made with the airfoils smooth because of the excessive roughness employed on the NACA airfoils. The largest value of  $c_{l,max}$ , 1.75, for the NACA airfoils was obtained for the forward-camber 230 airfoil series for a thickness ratio of 12 percent, which is probably the optimum thickness ratio. By contrast a value of  $c_{l,max}$  greater than 2 is shown for the NASA low-speed series for a thickness ratio of 13 percent. Large improvements in  $c_{l,max}$  performance for thickness ratios varying from 9 percent to 21 percent are shown for the NASA low-speed airfoils compared with the older NACA airfoils.

#### Refinements

21-percent-thick airfoil.- As previously discussed, the 21-percent airfoil displayed significantly lower values of lift-drag ratio compared to the thinner airfoils of the family because of turbulent boundary-layer separation at typical climb lift coefficients. Therefore, this thick airfoil has been reshaped to substantially decrease the upper-surface adverse pressure gradient and reduce the amount of separation on the airfoil. The changes in airfoil contour and pressure distribution are illustrated in figure 5. A theoretical analysis code with improved turbulent boundary-layer separation predictions (ref. 8) was used for the redesign of the airfoil. Note that the

start of the upper-surface pressure recovery was moved forward about  $0.30c$  for the modified airfoil. At a lift coefficient of  $0.40$  the theory indicates a decrease in the extent of upper-surface separation of about  $0.05c$  for the modified airfoil. Comparison of calculated and experimental pressure data indicate good agreement between experiment and theory for the modified airfoil. The experimental results were obtained in the Langley low-turbulence pressure tunnel.

Figure 6 compares lift-drag-ratio performance for the two airfoils for Reynolds numbers from  $2 \times 10^6$  to  $9 \times 10^6$ . At the design lift coefficient of  $0.40$  some improvement in lift-drag ratio is shown for the modified airfoil at a Reynolds number of  $2 \times 10^6$  even though there was no serious problem at this lift coefficient. However, at a typical climb lift coefficient of  $1.0$  large increases in lift-drag ratio are shown at all Reynolds numbers for the refined airfoil. The wind-tunnel results also indicated that the pitching-moment coefficient at design lift was reduced for the modified airfoil.

17-percent-thick airfoil.- Based on the significant increase in lift-drag ratio obtained for the redesigned 21-percent airfoil at typical climb lift coefficients, a redesign of the 17-percent airfoil was initiated. The objective of the redesign was twofold; to reduce the pitching-moment coefficient by increasing the forward loading and increase the climb lift-drag ratio by decreasing the aft upper-surface pressure gradient. The changes in airfoil contour and pressure distribution are illustrated in figure 7. A reduction in pitching-moment coefficient of about 28 percent is indicated by the theoretical calculations. Note that prior to the start of the aft upper-surface pressure recovery for the modified airfoil a flat pressure distribution or reduced pressure gradient region extends for about  $0.20c$ . This reduced pressure gradient region with the "corner" located at  $x/c = 0.60$  is considered to be an important feature of the airfoil design. Research reported in reference 9 for a modified 13-percent airfoil clearly indicated that this reduced pressure gradient region retards the rapid forward movement of upper-surface separation at the onset of stall and promotes docile stall behavior for airfoils which stall from the trailing edge. The chordwise location of the corner is determined by the aft pressure gradient which must be gradual enough to avoid separation at climb lift coefficients ( $c_l = 1.0$ ). Thus, the chordwise location of the corner is dependent on airfoil thickness ratio and design lift coefficient. The chordwise extent of the reduced pressure gradient region must be determined from experimental tests, since we are concerned with stall behavior. The theoretical separation points and pressure distributions for both 17-percent airfoils are shown in figure 8 at a climb lift coefficient of  $1.0$ . A reduction in the extent of separation of about  $0.05c$  is indicated for the modified airfoil. Based on these theoretical predictions some improvement in lift-drag ratio at  $c_l = 1.0$  would also be expected.

## MEDIUM-SPEED AIRFOILS

### Development

The design objective of the medium-speed airfoils was to increase the cruise Mach number of the low-speed airfoils but retain the good high-lift,

low-speed characteristics. Such new airfoils are intended to fill the gap between the low-speed airfoils and supercritical airfoils for application on light executive-type aircraft. Two medium-speed airfoils having thickness-chord ratios of 13 and 17 percent have been developed. The airfoils were designed for a lift coefficient of 0.30 and a Reynolds number of  $14 \times 10^6$ , and the design Mach numbers for the 13 and 17 percent airfoils were 0.72 and 0.68, respectively. The 13-percent medium-speed airfoil was obtained by reshaping the 13-percent low-speed airfoil as indicated in figure 9. The calculated pressure distribution shows that increasing the Mach number to 0.72 for the low-speed airfoil results in a region of high induced velocities near the midchord on the upper surface of the airfoil. Further increases in Mach number or lift coefficient would result in a shock wave developing on the airfoil. The airfoil has been reshaped to decrease the induced velocities near the midchord and increase the induced velocities in the forward region of the airfoil upper surface. The design criteria employed consisted of combining the best features of low-speed and supercritical airfoil technology for this application.

The design pressure distributions for both medium-speed airfoils are shown in figure 10. Note that the start of the aft upper-surface pressure recovery is located at about 0.50c for the 17-percent airfoil, compared with about 0.60c for the 13-percent airfoil. This is required in order to keep the aft pressure gradient gradual enough to avoid separation for the thicker airfoil. In order to retain good high-lift, low-speed characteristics for the new airfoils, the camber distribution was kept similar but not identical to the low-speed airfoil family.

#### Section Data

Low-speed section characteristics for the medium-speed airfoils are presented in figures 11 and 12 for a Reynolds number of  $4 \times 10^6$ . Comparison of the section data for the 13-percent low- and medium-speed airfoils (fig. 11) show that the stall characteristics for both airfoils are similar and that only a small decrease in  $c_{l,max}$  occurred for the medium-speed airfoil. Also, the pitching-moment coefficient has been decreased through the lift-coefficient range for the medium-speed airfoil. The drag polars for both airfoils are essentially the same. A similar comparison for the 17-percent low- and medium-speed airfoils (fig. 12) show no decrease in  $c_{l,max}$  and a decrease in drag coefficient at all lift coefficients for the medium-speed airfoil. Thus, the overall performance of the 17-percent medium-speed airfoil exceeds that for the earlier 17-percent low-speed airfoil. The small decrease in drag coefficient for the medium-speed airfoil at low lift coefficients is associated with the reduced aft upper-surface pressure gradient (fig. 13) and resulting boundary-layer development. The large decrease in drag coefficient at the higher lift coefficients for the medium-speed airfoil is a result of improved ability to design for and achieve less separation on the airfoil, as illustrated in figure 14 for a lift coefficient of 1.6. Turbulent trailing-edge separation is indicated by a region of nearly constant pressure upstream of the airfoil trailing edge.

The scale effects on maximum lift coefficient for the medium-speed airfoils for Reynolds numbers from about  $2 \times 10^6$  to  $9 \times 10^6$  are shown in figure 15. Increases in Reynolds number have a favorable effect on maximum lift coefficient for both airfoils. Application of roughness resulted in only a small decrease in  $c_{l,max}$  for both the 13- and 17-percent airfoils. Comparison of figures 3 and 15 for the 17-percent low- and medium-speed airfoils illustrate two interesting features. The irregular variation of  $c_{l,max}$  with Reynolds number at the lower Reynolds numbers and the sensitivity of  $c_{l,max}$  to roughness for the low-speed airfoil have been improved for the newer medium-speed airfoil design.

The effects of Mach number on maximum lift coefficient for the 13- and 17-percent low- and medium-speed airfoils are summarized in figure 16. The medium-speed airfoils generally show smaller decreases in  $c_{l,max}$  at the higher Mach number compared to the low-speed airfoils.

Theoretical calculated drag-rise characteristics (ref. 8) for the medium-speed airfoils at design conditions are shown in figure 17. Both airfoils indicate essentially no drag creep up to the design Mach numbers. The estimated drag-rise Mach numbers are about 0.76 and 0.72 for the 13- and 17-percent airfoils, respectively, which provide a margin of about 0.04 in Mach number above the design Mach numbers.

#### APPLICATIONS

Recently a number of United States general aviation manufacturers have announced the use of the NASA-developed low-speed airfoils on new aircraft; these are summarized as follows:

<u>Aircraft</u>	<u>Airfoil</u>
Hustler (American Jet)	Modified LS(1)-0413, formerly GA(W)-2
Model 77 (Beech)	LS(1)-0417, formerly GA(W)-1
Model 303 (Cessna)	LS(1)-0413
PA-38 Tomahawk (Piper)	LS(1)-0417

#### CONCLUDING REMARKS

An initial family of low-speed airfoils for general aviation applications has been investigated. These airfoils provide significant improvements in maximum lift coefficients compared to the older NACA airfoils. Refinements to the 17-percent low-speed airfoil to reduce the pitching-moment coefficient and to the 21-percent low-speed airfoil to increase the lift-drag ratio have been completed. Two medium-speed airfoils with thickness ratios of 13 and 17 percent have been developed. These new airfoils provide increased cruise Mach numbers

over the low-speed airfoils, while retaining good high-lift, low-speed characteristics. The NASA-developed low-speed airfoils are now being used by several United States general aviation manufacturers.

Langley Research Center  
National Aeronautics and Space Administration  
Hampton, VA 23665  
February 8, 1979

#### REFERENCES

1. Stevens, W. A.; Goradia, S. H.; and Braden, J. A.: Mathematical Model for Two-Dimensional Multi-Component Airfoils in Viscous Flow. NASA CR-1843, 1971.
2. McGhee, Robert J.; and Beasley, William D.: Low-Speed Aerodynamic Characteristics of a 17-Percent-Thick Airfoil Section Designed for General Aviation Applications. NASA TN D-7428, 1973.
3. McGhee, Robert J.; and Beasley, William D.: Effects of Thickness on the Aerodynamic Characteristics of an Initial Low-Speed Family of Airfoils for General Aviation Applications. NASA TM X-72843, 1976.
4. Wentz, W. H., Jr.; and Seetharam, H. C.: Development of a Fowler Flap System for a High Performance General Aviation Airfoil. NASA CR-2443, 1974.
5. Wentz, W. H., Jr.: Effectiveness of Spoilers on the GA(W)-1 Airfoil With a High Performance Fowler Flap. NASA CR-2538, 1975.
6. Wentz, W. H., Jr.: Wind Tunnel Tests of the GA(W)-2 Airfoil With 20% Aileron, 25% Slotted Flap, 30% Fowler Flap, and 10% Slot-Lip Spoiler. NASA CR-145139, 1977.
7. Gregorek, G. M.; Hoffmann, M. J.; Weislogel, G. S.; and Vogel, G. M.: In-Flight Measurements of the GA(W)-2 Aerodynamic Characteristics. [Preprint] 770461, Soc. Automot. Eng., Mar.-Apr. 1977.
8. Bauer, Frances; Garabedian, Paul; Korn, David; and Jameson, Antony: Supercritical Wing Sections II. Volume 108 of Lecture Notes in Economics and Mathematical Systems, Springer-Verlag, 1975.
9. McGhee, Robert J.; and Beasley, William D.: Low-Speed Wind-Tunnel Results for a Modified 13-Percent-Thick Airfoil. NASA TM X-74018, 1977.

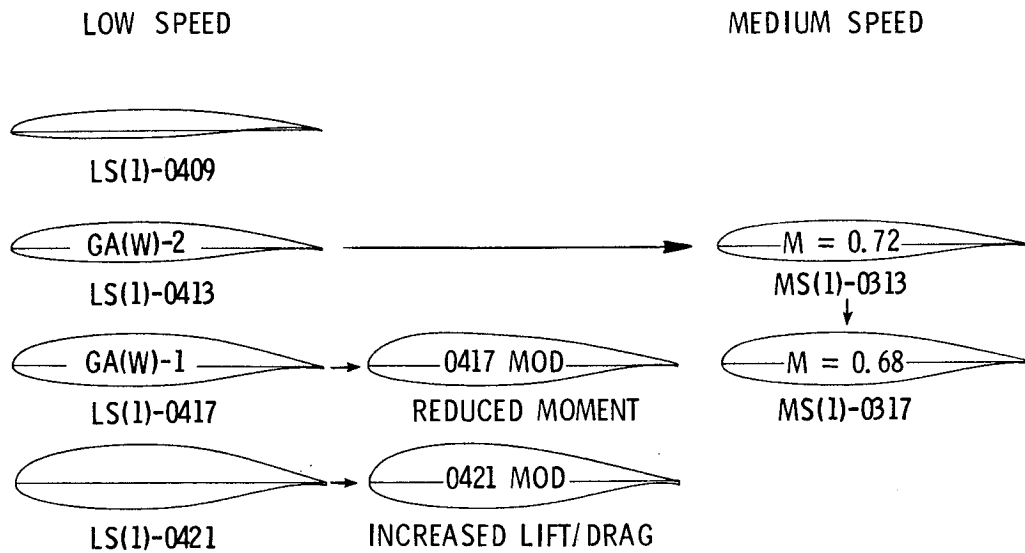


Figure 1.- Section shapes and airfoil designations for NASA low- and medium-speed airfoils.

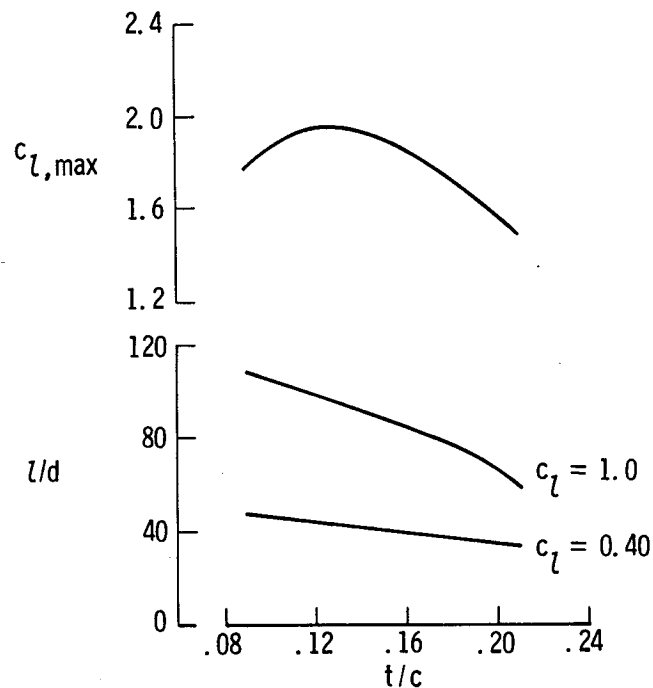


Figure 2.- Effect of airfoil thickness ratio on  $c_{l,max}$  and lift-drag-ratio performance for low-speed airfoils.  $M = 0.15$ ;  $R = 4 \times 10^6$ ;  $(x/c)_T = 0.075$ .

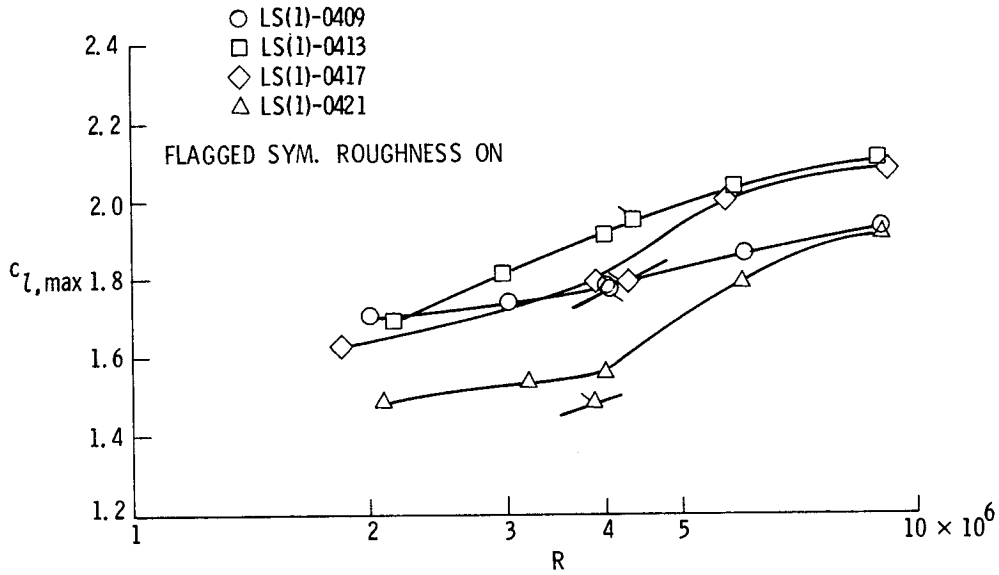


Figure 3.- Effect of Reynolds number on  $c_{l,max}$  for low-speed airfoils.  
 $M = 0.15$ .

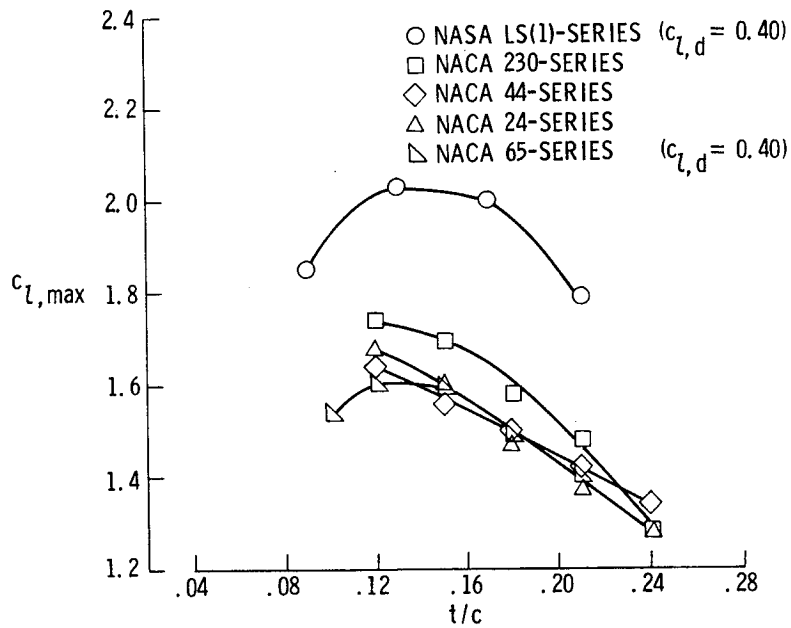


Figure 4.- Comparison of  $c_{l,max}$  of NASA low-speed airfoils and NACA airfoils.  
 $M = 0.15$ ;  $R = 6 \times 10^6$ ; airfoils smooth.

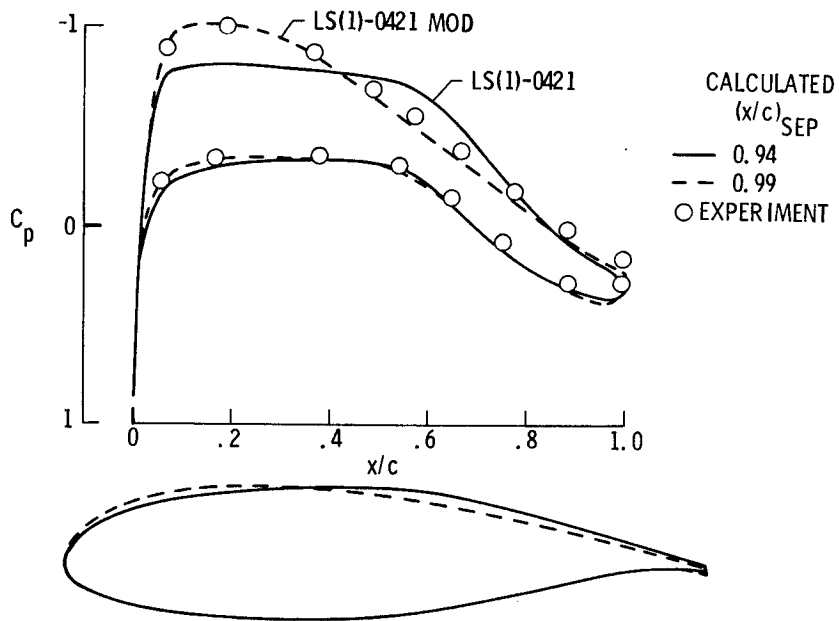


Figure 5.- Pressure distributions for 21-percent low-speed airfoils.  
 $M = 0.15$ ;  $R = 4 \times 10^6$ ;  $c_l = 0.40$ .

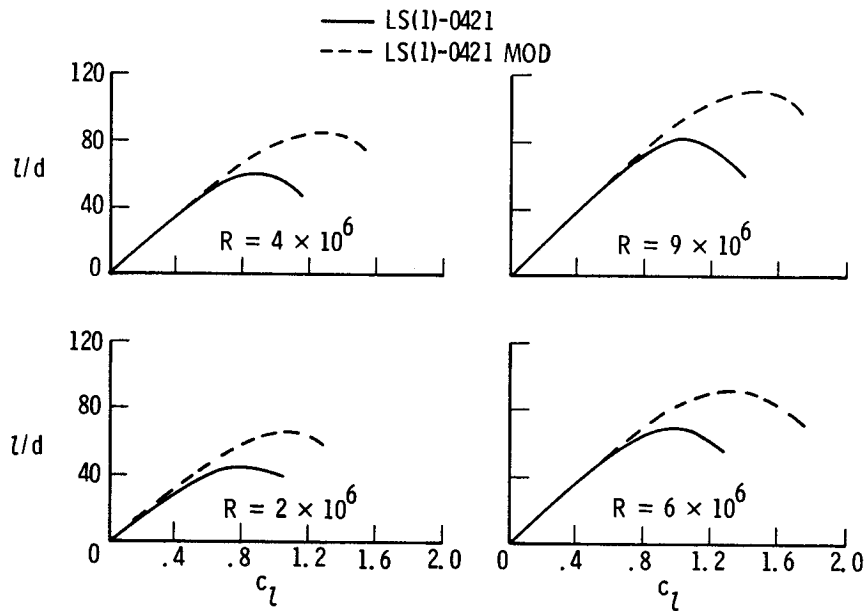


Figure 6.- Comparison of experimental lift-drag-ratio performance for 21-percent low-speed airfoils.  $M = 0.15$ ;  $(x/c)_T = 0.075$ .



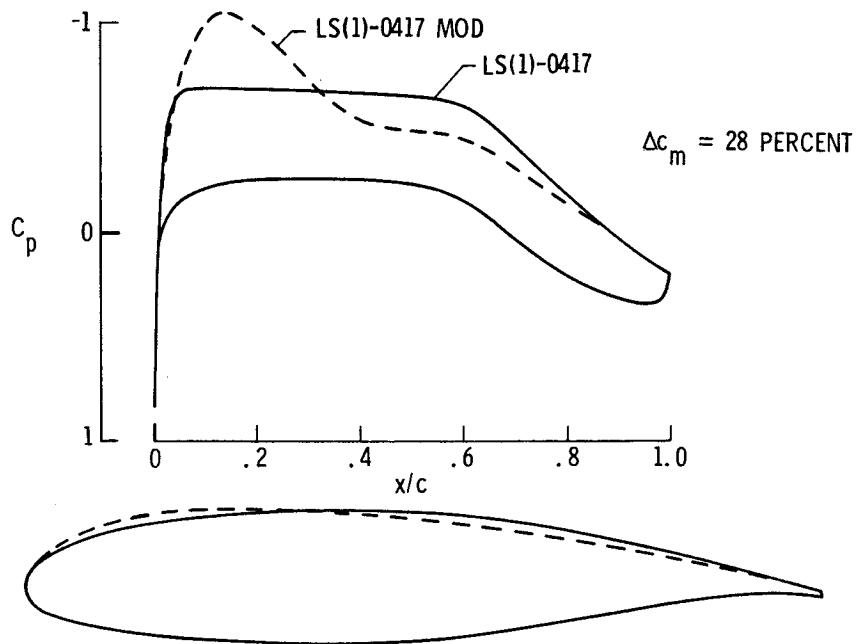


Figure 7.- Calculated pressure distributions for 17-percent low-speed airfoils.  
 $M = 0.15$ ;  $R = 4 \times 10^6$ ;  $c_l = 0.40$ .

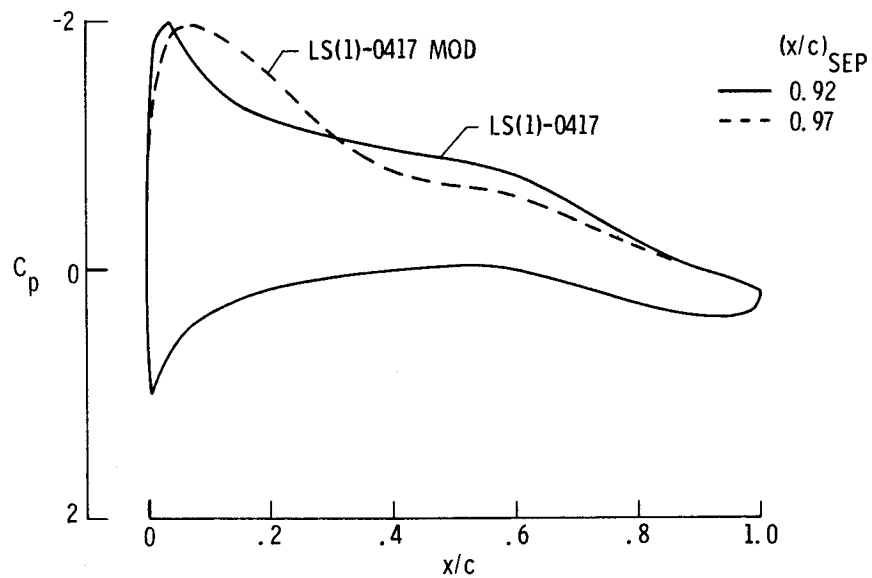


Figure 8.- Calculated pressure distributions and separation points for 17-percent low-speed airfoils.  $M = 0.15$ ;  $R = 4 \times 10^6$ ;  $c_l = 1.0$ .

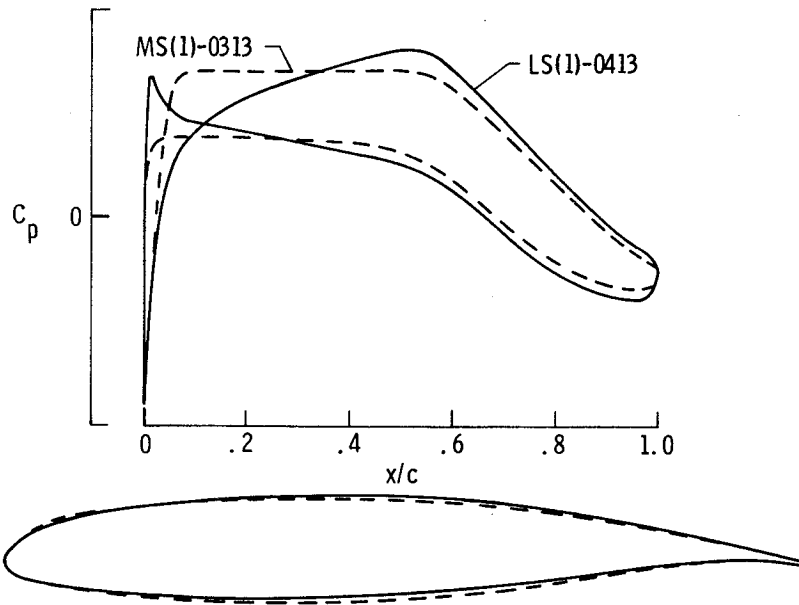


Figure 9.- Calculated pressure distributions for 13-percent low- and medium-speed airfoils.  $M = 0.72$ ;  $R = 14 \times 10^6$ ;  $c_l = 0.30$ .

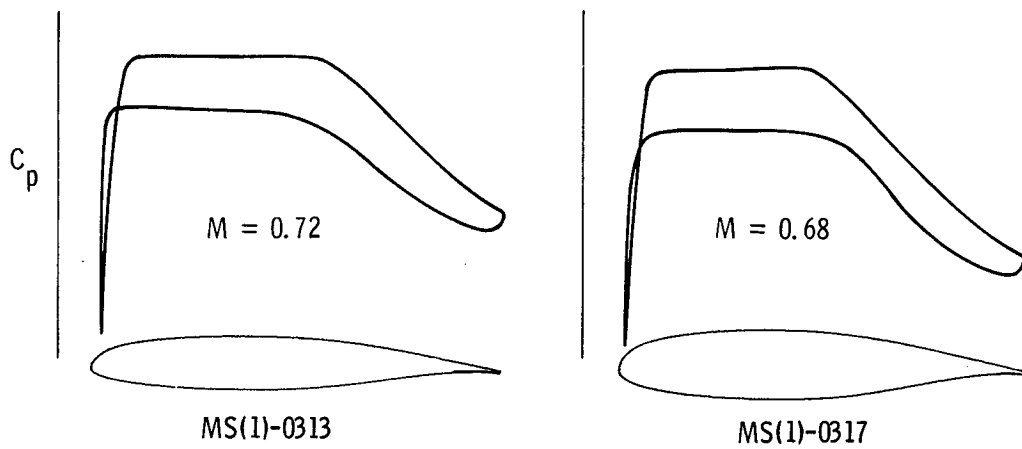


Figure 10.- Calculated design pressure distributions for 13- and 17-percent medium-speed airfoils.  $R = 14 \times 10^6$ ;  $c_l = 0.30$ .

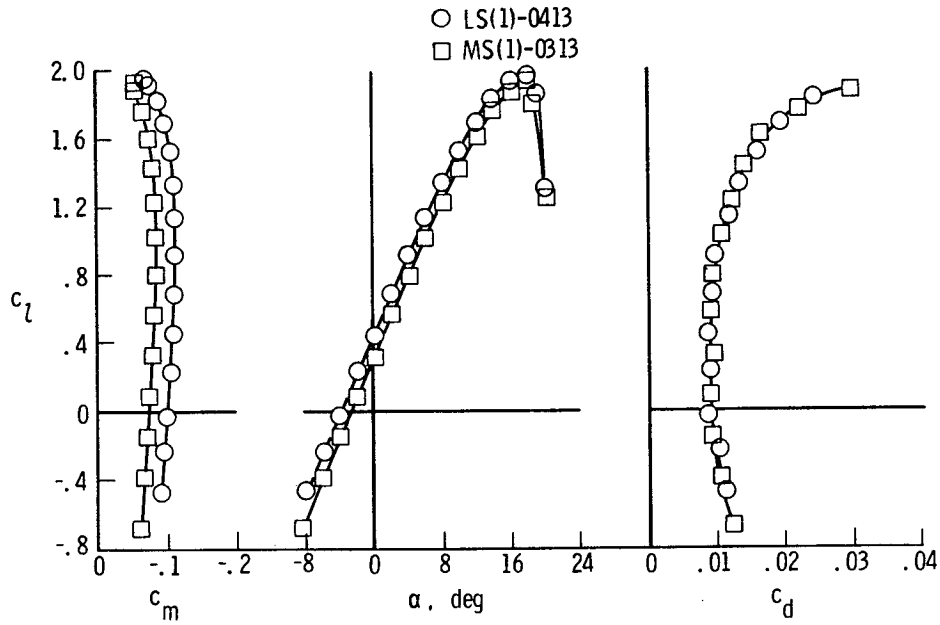


Figure 11.- Section data for 13-percent low- and medium-speed airfoils.  
 $M = 0.15$ ;  $R = 4 \times 10^6$ ;  $(x/c)_T = 0.075$ .

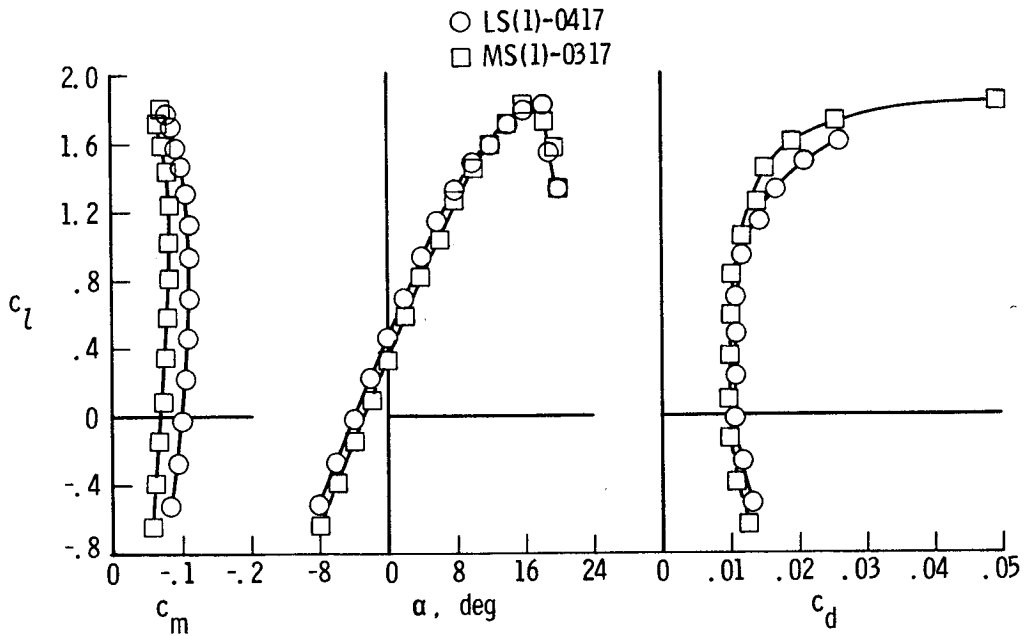


Figure 12.- Section data for 17-percent low- and medium-speed airfoils.  
 $M = 0.15$ ;  $R = 4 \times 10^6$ ;  $(x/c)_T = 0.075$ .

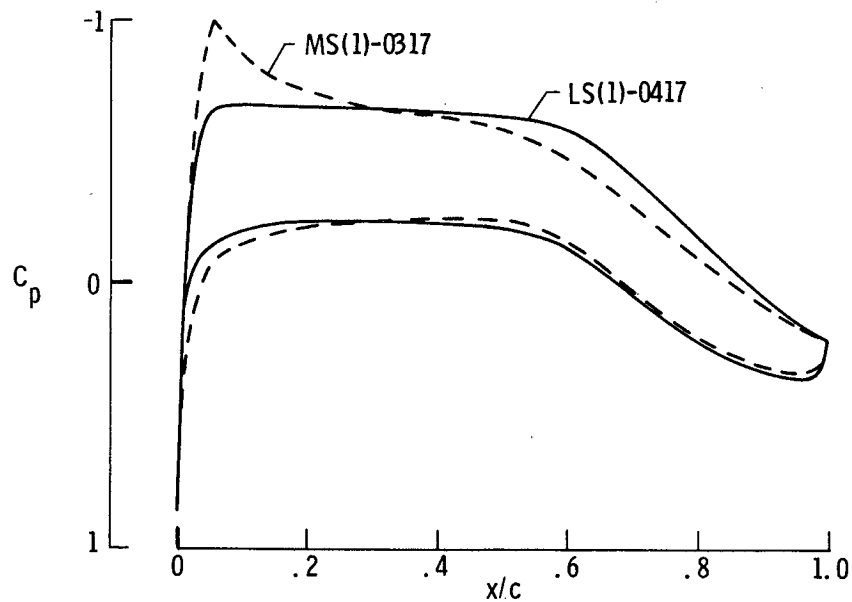


Figure 13.- Calculated pressure distributions for 17-percent low- and medium-speed airfoils.  $M = 0.15$ ;  $R = 4 \times 10^6$ ;  $c_l = 0.40$ .

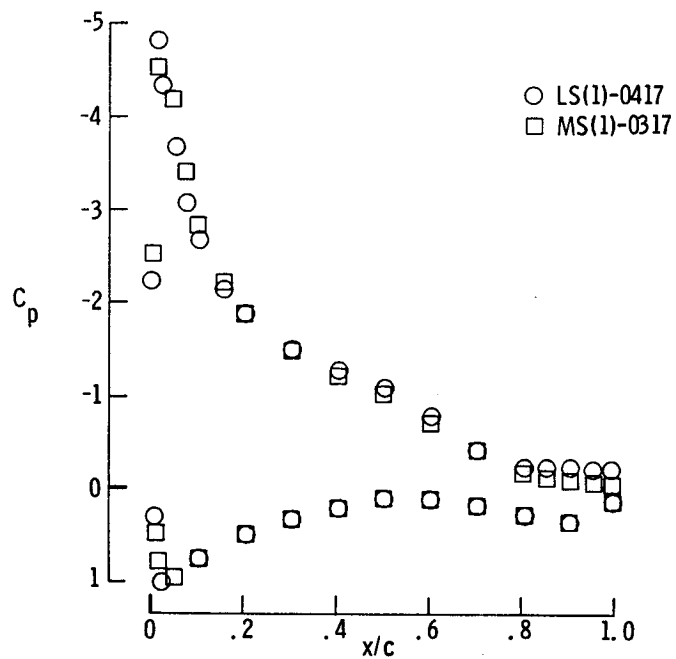


Figure 14.- Experimental pressure distributions for 17-percent low- and medium-speed airfoils.  $M = 0.15$ ;  $R = 4 \times 10^6$ ;  $c_l = 1.6$ .

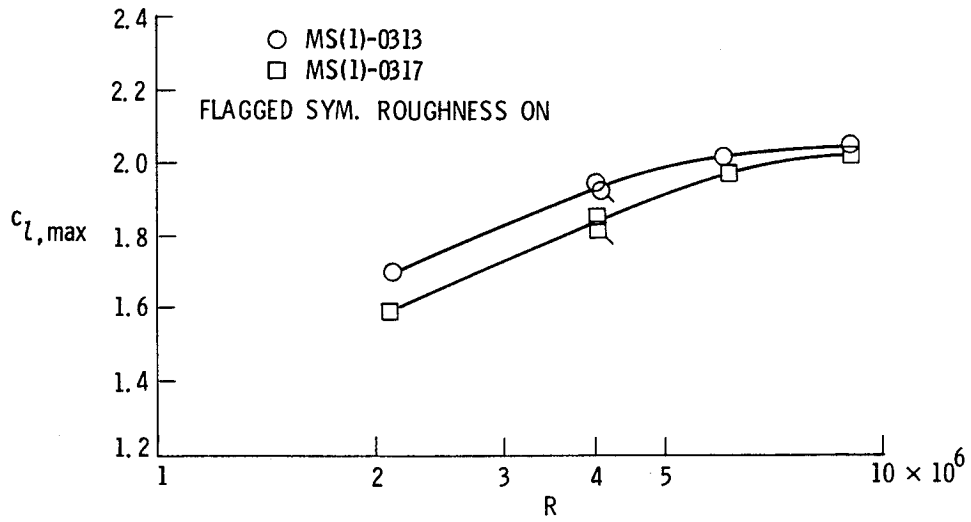


Figure 15.- Effect of Reynolds number on  $c_{l,max}$  for medium-speed airfoils.  
 $M = 0.15$ .

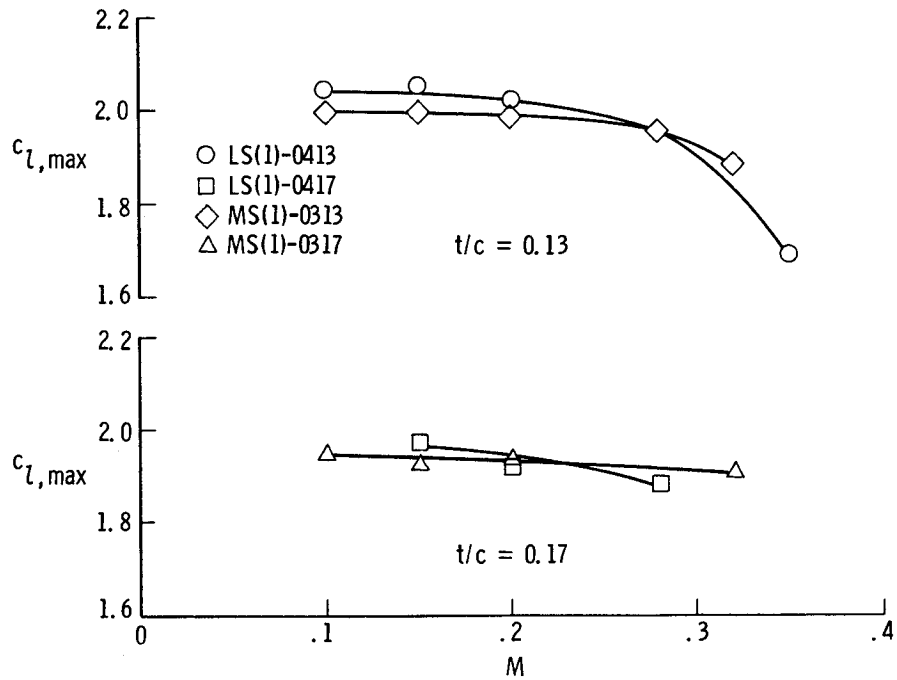


Figure 16.- Effect of Mach number on  $c_{l,max}$  for low- and medium-speed airfoils.  $R = 6 \times 10^6$ ;  $(x/c)_T = 0.075$ .

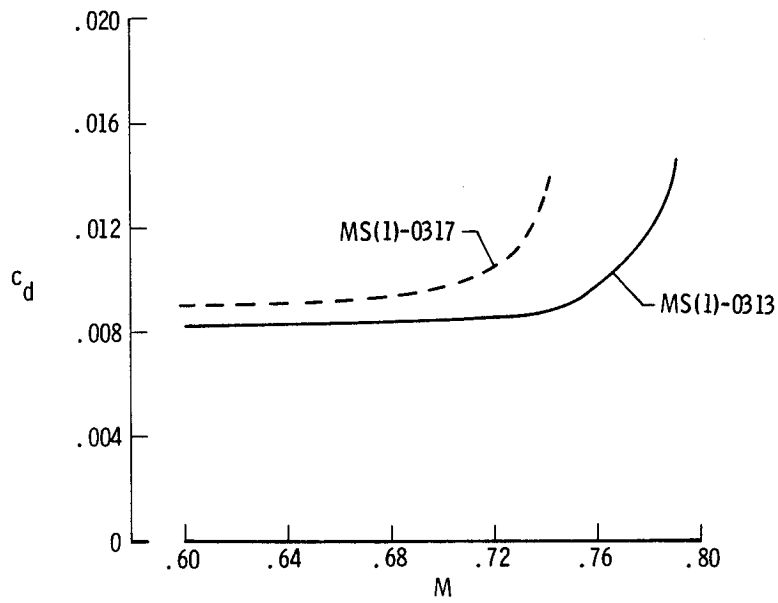


Figure 17.- Calculated drag-rise characteristics for medium-speed airfoils.  
 $R = 14 \times 10^6$ ;  $c_l = 0.30$ .